


Hot corrosion behaviors of as-sprayed and laser-remelted YSZ thermal barrier coatings at 950 °C

Z.G. Yang^{1,2*} , W.P. Liang^{2*}, Q. Miao²,
Z. Ding², B.Z. Huang²

¹Anyang Institute of Technology, School of Mechanical Engineering, West section of Yellow River Avenue, 455000, Anyang, China.

²Nanjing University of Aeronautics and Astronautics, School of Materials Science and Technology, 29 General Avenue, 211100, Nanjing, China.

e-mail: 438099980@qq.com, wpliange@nuaa.edu.cn, miaoqiang@nuaa.edu.cn, dingzheng0126@163.com, 1214620170@qq.com

ABSTRACT

In the current study, the influences of laser remelting treatment on NiCoCrAlY/ZrO₂-7 wt.% Y₂O₃ thermal barrier coatings fabricated via plasma spraying on GH4169 alloy were examined. The microstructure, microhardness, hot corrosion resistance at 950 °C of the two types of TBCs were investigated comparatively. The results indicated that the as-sprayed TBCs had a lamellar structure with high cracks and porosity. After laser remelting treatment, a laser remelted layer with a compact sub-micro sized grains arranged in a stacked structure was formed which was denser than that of the as-sprayed TBCs. The surface microhardness of the as-sprayed TBC was only 977 HV_{0.3}, which exhibited a significant increase (over 1500 HV_{0.3}) after laser remelting due to the fine grains of the remelted region with lower porosity. The hot corrosion resistance of the laser remelted TBCs were considerably better than the as-sprayed one. The as-sprayed TBC with a lot of defects, the molten salts could easy penetrate the coating and react with Y₂O₃. The consumption of Y element promoted the phase transition of t'-ZrO₂ to m-ZrO₂, which harmed the protective coating because of the volume expansion of the phase transition. The laser remelted TBCs was dense, which could significantly reduce the penetrate of molten salts due to the fewer cracks and holes compared to the as-sprayed TBCs. The laser remelted TBCs exhibited superior hot corrosion performance as compared to the as-sprayed TBCs.

Keywords: Thermal barrier coatings; Laser remelted; Hot corrosion; Ytria-stabilized zirconia; Nickel-based superalloy.

1. INTRODUCTION

Ni-based superalloys have been widely used extensively in aerospace industry due to the high hardness and strength of it under high temperatures [1, 2]. With the development of technological, the demands for aero-engine performance are increasing. The engine operating temperatures have become increasingly high to reduce fuel consumption and improve work efficiency [3]. Therefore, the protective coatings for Ni-based superalloy components to improve the application temperature are necessary.

Thermal barrier coatings (TBCs) are popularly used in many hot section parts to protect metallic parts against the high temperature degradations and enhance the service life of it [4]. A typical TBC system consists of a thermally insulating ceramic top coating and an oxidation-resistant metallic bond coating. The MCrAlY (M=Ni and/or Co) alloys are the best choice for bond coating because of enabling selective the formation of alumina and good adherence [5]. The ZrO₂ is the most suitable overlay coating for the top ceramic coating due to the excellent chemical stability and low thermal conductivity of it [6].

TBCs could be exposed to degradation during the application environment such as corrosion, oxidation, CaO-MgO-Al₂O₃-SiO₂ (CMAS) attack and so on [7]. The hot corrosion on the ceramic top layer occurs because of the adhering fuel impurities, which react with ceramic layer. The formation of new phases reduces the stability of the ceramic layer [8]. Furthermore, the oxygen passes through the ceramic top layer and oxidizes the metallic bond layer during the high temperature service conditions. The thermally grown oxide (TGO) layer forms between the top and bond layer, which damages TBCs generally [9].

In the last decades, a variety of methods can fabricate TBCs such as plasma spraying, and electron beam-physical vapor deposition [10–12]. Plasma spraying is one of the main methods for preparing TBCs due to the high efficiency and easy to control the coating thickness [13]. However, TBCs fabricated by plasma spraying have many defects such as high volume porosity, typical lamellar microstructure and high surface roughness. These defects can damage the coating and reduce the service life of it under the harsh environment. Thus, there is an interest in densifying the TBCs surface. The dense layer increases the competitive level of TBCs, which is expected to eliminate the pores and cracks on the surface of the as-sprayed coating. Yan Wang *et al.* [14] pointed out that the laser remelted YSZ TBCs could improve the cavitation erosion resistance because the laser remelting produces a dense layer with few cracks. X.F. Zhang *et al.* [15, 16] reported that a Al_2O_3 film was prepared on YSZ TBCs to against CMAS corrosion. However, the dense Al_2O_3 layer was thin and could be easily damaged.

In the present study, $\text{NiCoCrAlY/ZrO}_2\text{-7wt\%Y}_2\text{O}_3$ TBCs were deposited on GH4169 alloy by plasma spraying. Afterwards, the as-sprayed TBCs were post-treated by laser remelting process with a CO_2 laser. The microstructure, microhardness, the performance under the hot corrosion tests at 950 °C of the two types of TBCs were examined comparatively.

2. MATERIALS AND METHODS

The GH4169 alloy (provided by Beijing Institute of Aerial Materials of China) with the chemical composition of 52.4Ni-18.4Cr-5.5Nb-3.2Mo-1.4Co-18.2Fe-0.9Ti (wt%) was chosen as the substrate material, which was cut into 10 mm × 10 mm × 4 mm by wire cutting. All samples were grit blasted by Al_2O_3 powders ($40 \pm 5 \mu\text{m}$ particle size) under the 2.5 bar pressure condition, then cleaned in ethanol to remove contamination.

The Ni-25Co-18Cr-10Al-Y metallic powders (purchased from Zhongzhou Special Alloy Materials Co., Ltd.) with the size range of 30–85 μm were used to prepare the bond coat, as presented in Figure 1a. The YSZ ($\text{ZrO}_2\text{-7wt.\%Y}_2\text{O}_3$) ceramic powders (purchased from Jinzhou Jinjiang Spraying Material Co., Ltd.) with the size range of 25–80 μm were used to fabricate the top coat, as shown in Figure 1b. TBCs were fabricated by atmospheric plasma spraying (Praxair, 100HE, USA), the experimental parameters were listed in Table 1. The laser surface remelting treatment was performed by 2-kW CO_2 laser (PRIMA INDUSTRIE S.P.A, SLCF-12 × 25, China), which blown argon with a flow of 5 L/min to prevent the oxidation. The parameters of laser surface remelting treatment were as follows: the laser beam output power was 550 W, the laser beam moving speed was 350 mm/min with a 3 mm × 3 mm dimension laser spot.

The morphologies of as-sprayed and laser remelted TBCs were analyzed by emission scanning electron microscopy (Hitachi, S-4800, Japan). An X-ray diffraction (Bruker, D8-ADVANCE, Germany) with copper $\text{K}\alpha$ radiation ($\lambda = 1.5418 \text{ \AA}$) was applied for the phase analysis. The micro-hardness of as-sprayed and laser remelted TBCs was examined by Vickers Indenter (DianYing, DHV-1000/Z, China) with 300 g load lasting 15 s. The surface roughness of the coating was analyzed via a MicroXAMTM 3D Profiler (ADEPhase-shift, USA). The porosity of the coating was analyzed by magnifying five random sections 200 times using a MA-200 optical microscope (Nikon, Japan). The coating porosity images were changed into black-and-white two-value images through the threshold method. Hot corrosion tests were also examined. By weight 75% Na_2SO_4 and 25% NaCl mixed powders were spread onto the surface of TBCs at approximately 2 mg/cm². Samples were then put in electric furnace (Protherm, PLF 130/12, Turkey) at 950 °C for 100 h. The mass changes were calculated by sensitive electronic scale (JingKe, FA1044, China).

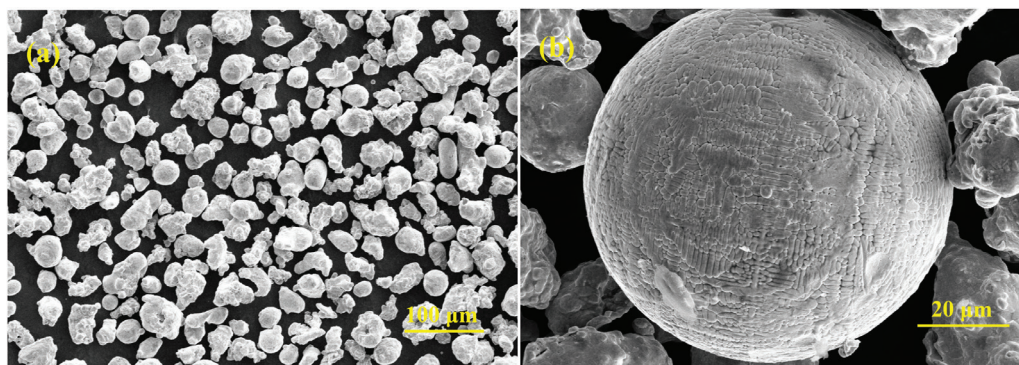


Figure 1: SEM images (a) Ni-25Co-18Cr-10Al-Y metallic powders (b) $\text{ZrO}_2\text{-7wt.\%Y}_2\text{O}_3$ powders.

Table 1: The experimental parameters of TBCs by atmospheric plasma spraying.

| Parameter | Bonding coat | Ceramic coat |
|------------------------------------|--------------|--------------|
| Voltage (V) | 65 | 75 |
| Current (A) | 500 | 510 |
| Thickness (μm) | 90–100 | 190–200 |
| Spray speed (mm/s) | 600 | 600 |
| Spray distance (mm) | 110 | 110 |
| Ar powder flow (L/min) | 65 | 50 |
| N ₂ powder flow (L/min) | 15 | 15 |
| H ₂ powder flow (L/min) | 6 | 6 |
| Powder speed (g/min) | 50 | 15 |

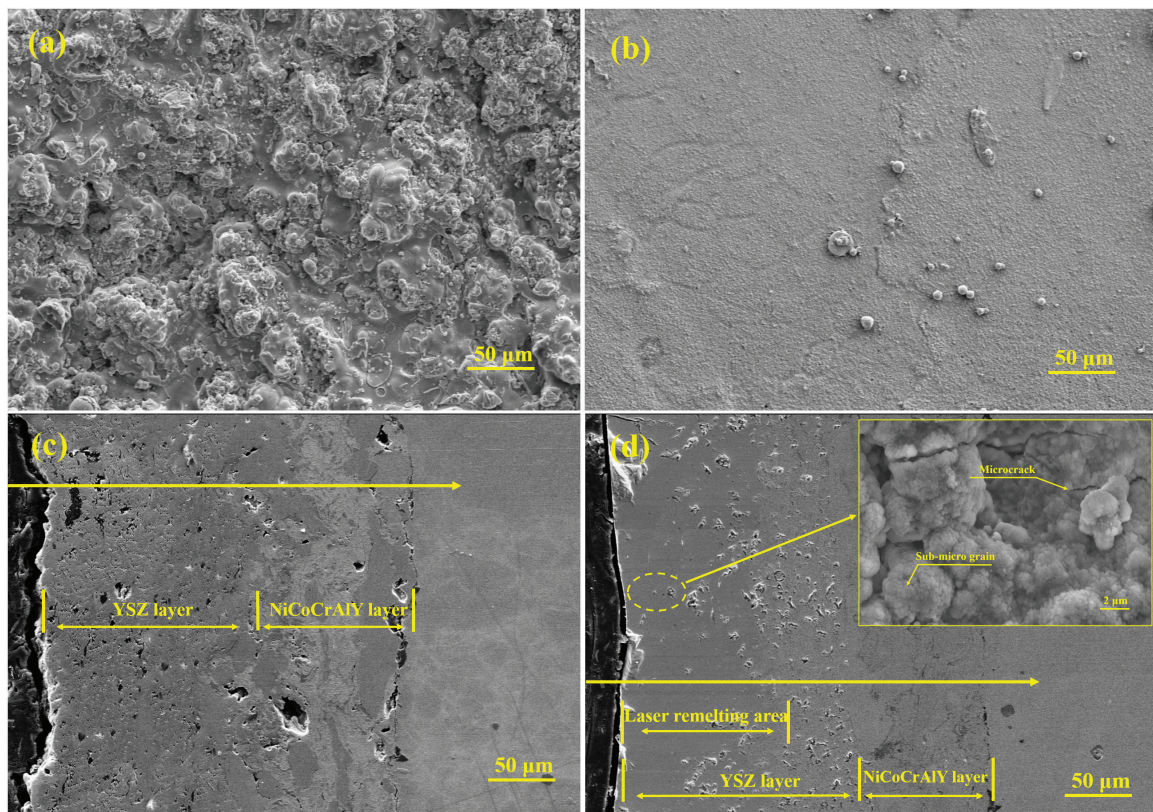


Figure 2: SEM images of as-sprayed and laser remelted TBCs (a) surface of as-sprayed coating (b) surface of laser remelted coating (c) cross-section of as-sprayed coating (d) cross-section of laser remelted coating.

3. RESULTS AND DISCUSSION

3.1. Characteristic of as-sprayed and laser remelted TBCs

Figure 2a and b shows the surface SEM images of both as-sprayed and laser remelted TBCs. In as-sprayed TBC, the typical plasma sprayed surface is identifiable. The coating represents a few pores and incomplete melted feedstock, which cause extremely rough surface ($R_a = 12.1 \mu\text{m}$). As for laser remelted TBC, the laser remelting treatment smoothens the top ceramic layer and reduces the surface roughness exceedingly ($R_a = 2.7 \mu\text{m}$). The laser remelted layer is considerable denser and has no obvious defects, there are only a few sputtered laser

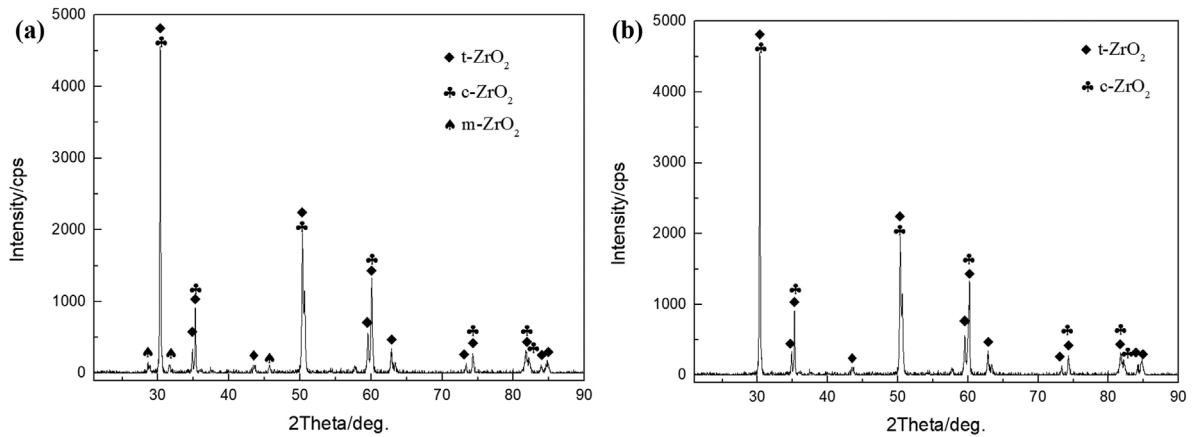


Figure 3: XRD patterns (a) the as-sprayed TBCs (b) the laser remelted TBCs.

remelted TBC particles on it during laser remelting. The slight cracks appear on it due to the uneven thermal stress distribution, which attributes to the high cooling rate of the molten pool [17]. The crack generation is a main problem for laser remelting. However, laser remelting has exhibited the potential to improve the performance of as-sprayed TBC by eliminating porosity and smoothing the top layer [18].

The cross-sectional SEM image of as-sprayed TBC is presented in Figure 2c. The ceramic top layer, metallic bond layer and substrate exist in turn from the surface to the inside. There are a certain number of pores and cracks present in as-sprayed TBCs. The porosity of as-sprayed TBC is mostly 12.42%. The top ceramic layer has a lamellar structure, which attributes to the accumulating flattened splats during the plasma spray treatment [19]. Sobhanverdi *et al.* reported that the sprayed process has effect on the porosity of the TBCs. The higher porosity of the TBCs is beneficial to the thermal conductivity and the thermal shock resistance [20, 21]. However, the higher porosity of the TBCs is bad to the mechanical property of the TBCs, the thermal stress caused by the rapid solidification of feedstock easily lead to the formation of cracks. The cross-sectional SEM of laser remelted TBC (Figure 2d) exhibits a very different microstructure from the as-sprayed TBC. The result indicates that the top ceramic layer cannot be remelted completely after laser remelting processing, which attributes to the significant thickness and the low thermal conductivity of the ceramic layer. The porosity of laser remelted TBC is 4.34%, which is only 34.9% of the original coating. During the laser remelting treatment, although the molten pool solidified quickly, the pores in the surface TBC had enough time to rise away. The laser remelting area consists of compact sub-micro sized grains arranged in a stacked structure and a few microcracks exist between the deposited particles in it (Figure 2e), which attribute to the temperature gradient and the solidification rate of the molten pool. Thus, the laser remelting area is dense and free of pores, which contributes to improve the hot corrosion resistance.

Figure 3 shows the XRD patterns of the as-sprayed and laser remelted TBCs. According to the XRD analysis, the peaks of as-sprayed TBC caused by cubic zirconia (c-ZrO₂) and monoclinic zirconia (m-ZrO₂) as well as the prominent peak of metastable tetragonal zirconia (t'-ZrO₂), which is very similar to the reported by C. Batista *et al.* [22]. During the plasma spraying treatment, the powder phases transformed into t'-ZrO₂ and c-ZrO₂ due to the heating and melting. Then some of c-ZrO₂ transformed into t'-ZrO₂ and partial t'-ZrO₂ transformed into m-ZrO₂ due to the inadequate content of the Y₂O₃ during the feedstock (with high speed and temperature) impacted and solidified on the surface of substrate. Therefore, the formation of m-ZrO₂ is limited. As for laser remelted TBC, the diffraction peaks are slightly different. Only t'-ZrO₂ and c-ZrO₂ phases appear after laser remelting treatment, the t'-ZrO₂ transform into m-ZrO₂ was inhibited due to the higher cooling rate during laser remelting treatment [14]. Therefore, the peaks of m-ZrO₂ phase were not to be found in laser remelted TBC because of the content of m-ZrO₂ is extremely low. In general, the phase transformation of m-ZrO₂ can lead to the volumetric changes and cause cracks formation in top ceramic layer [23]. The laser remelting treatment inhibits the phase transformation, which is beneficial to the performance of the TBCs.

The microhardness profiles of the as-sprayed and laser remelted TBCs along the depth direction are exhibited in Figure 4. The results indicate that the surface microhardness of the as-sprayed TBC is only 977 HV_{0.3}, which exhibits a significant increase (over 1500 HV_{0.3}) after laser remelting. The microhardness of laser remelted TBC is much higher than that of as-sprayed TBC, which can be attributed to the fine grains of the remelted region with lower porosity [24]. The laser remelting area consists of compact sub-micro sized grains arranged in a stacked structure, which is denser than the as-sprayed coating with a large number of pores and

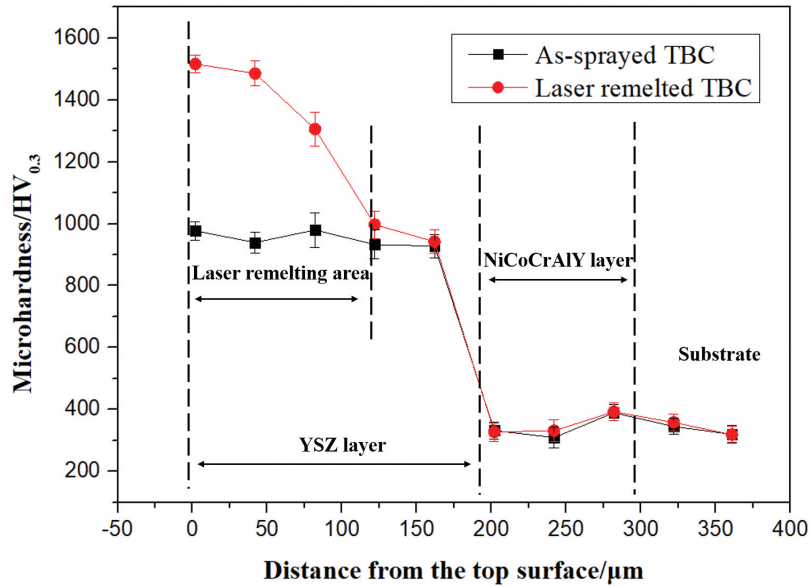


Figure 4: Microhardness distributions of the as-sprayed and laser remelted TBCs along the depth direction.

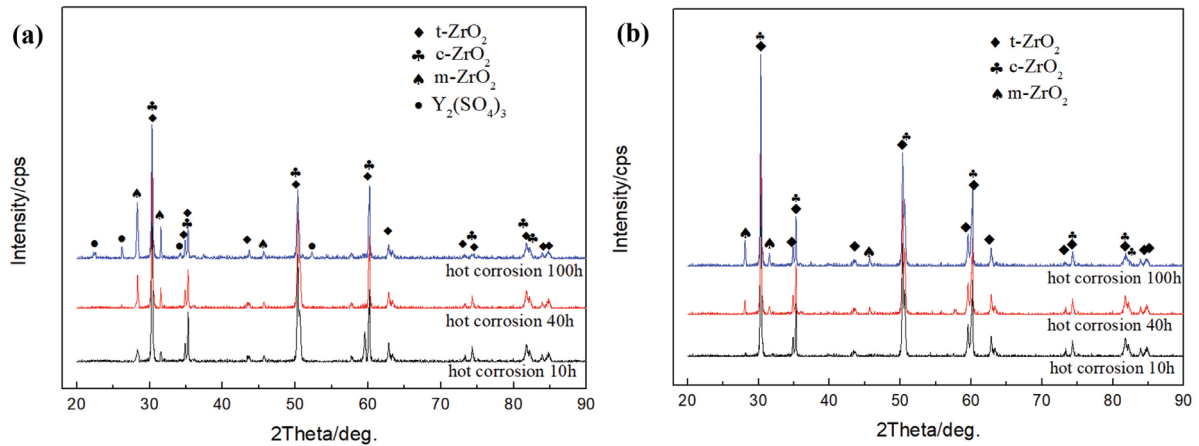


Figure 5: XRD patterns after hot corrosion test (a) the as-sprayed TBCs (b) the laser remelted TBCs.

cracks. Furthermore, the microhardness of the laser remelted TBC gradually decreases from the coating surface to the substrate, the hardness value is similar to the as-sprayed TBC one in the metallic bond layer region. The results are consistent with the SEM analysis, the laser remelted top ceramic layer consists of the remelted region and remained as-sprayed region. As for both the as-sprayed and laser remelted TBC, the microhardness of the substrate close to the metallic bond layer is slightly higher than original substrate microhardness (around 280–300 HV_{0.3}), which is attributed to the hardening treatment by plasma spraying.

3.2. Hot corrosion characteristics of as-sprayed and laser remelted TBCs

The hot corrosion tests were carried out in the laboratory environment at 950 °C for 10 h, 40 h and 100 h, respectively. The mixed powders of 75% Na₂SO₄ and 25% NaCl (by weight) were spread onto surface of samples. The XRD patterns of the as-sprayed and laser remelted TBC after the hot corrosion tests are shown in Figure 5. As for the as-sprayed TBC, the peaks caused by the main t'-ZrO₂ and c-ZrO₂ phases, a few m-ZrO₂ phases were also detected. With the extension of corrosion time, the peaks of m-ZrO₂ phases were significantly increased and the t'-ZrO₂ phases were decreased at the same time. The slightly peaks of Y₂(SO₄)₃ appeared at the later stage of corrosion. Vassen *et al.* [25] pointed that the Y₂O₃ has the effect of stabilizing the ZrO₂. Based on the products of the as-sprayed TBC after hot corrosion tests, it can be concluded that the reduction of Y₂O₃ content promotes the phase transfer of ZrO₂ phases. The results suggested that the volume fraction of m-ZrO₂ increases as well as the volume fraction of t'-ZrO₂ decreases, which proves that the phase transition of t'-ZrO₂ to m-ZrO₂ occurs during the hot corrosion test. Figure 5b shows the XRD patterns of laser remelted TBC after hot

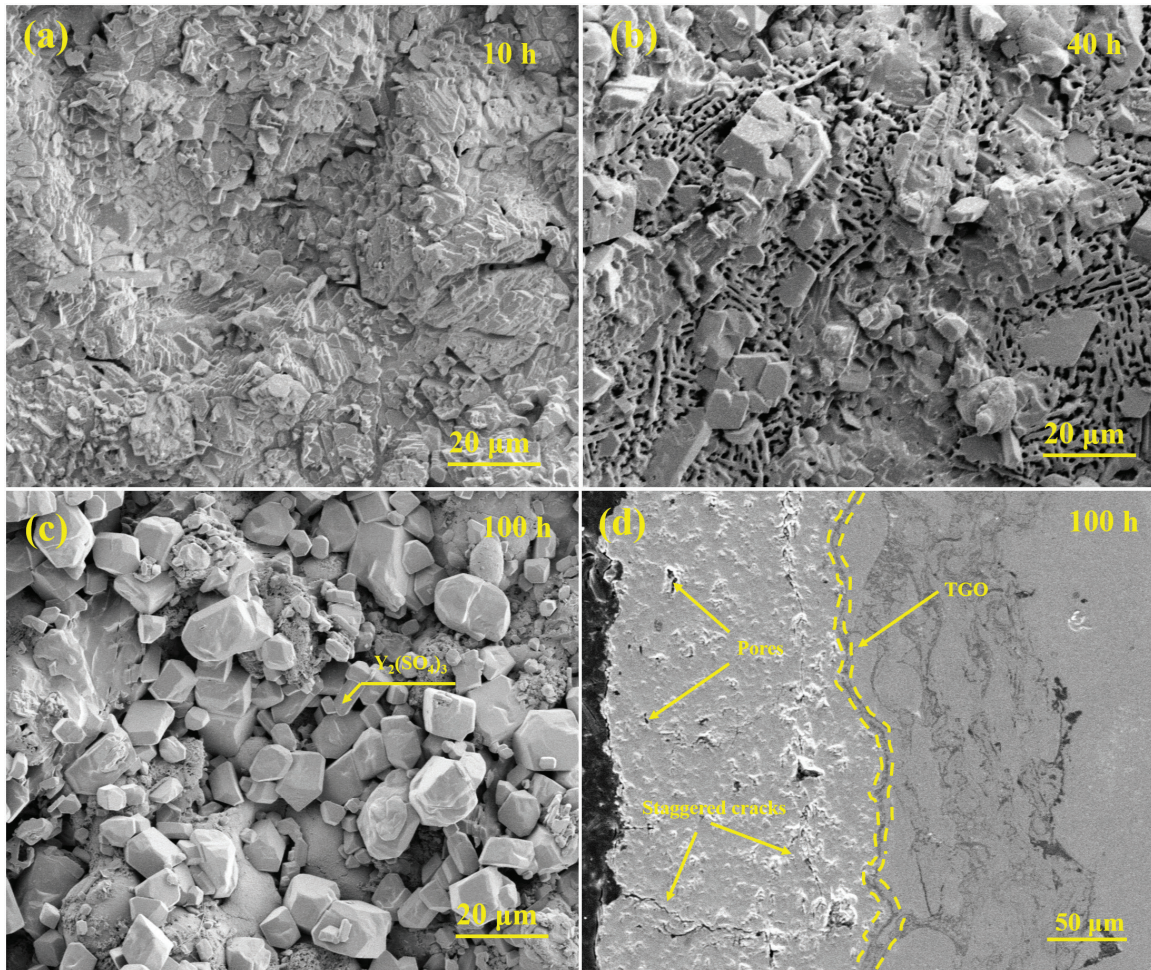


Figure 6: SEM images of the as-sprayed TBC after hot corrosion test (a) 10 h (b) 40 h (c) 100 h and (d) cross-section.

corrosion tests, the peaks caused by t' -ZrO₂, c-ZrO₂ and m-ZrO₂ phases. There are no Y₂(SO₄)₃ phase appeared in the pattern after 100 h hot corrosion test. The results suggested that laser remelting treatment improves the stability of TBC, which reduces the inadequate content of Y₂O₃ and makes the TBC dense. The uniformly distributed of Y₂O₃ inhibits the phase transition of t' -ZrO₂ to m-ZrO₂. In general, the content of the phase is above 5%, which could be detected accurately via XRD technology. The content of Y₂(SO₄)₃ products is very low with undetected by XRD after hot corrosion test due to the dense and uniform of the top ceramic layer. The laser remelted TBC exhibits great corrosion resistance after 100 hot corrosion tests at 950 °C.

In Figure 6, the SEM images belonging to as-sprayed TBC after the hot corrosion tests are given. The results suggested that the surface microstructure became loose, some voids and cracks appeared on it after 10 h hot corrosion test. The corrosion products were small and dispersed on the surface, which stated to form with the nucleation from the early stage of corrosion. With the extension of corrosion time, there were large number of mesh connection structures appeared between the particles, the particle size had a certain degree of increase compared to that in the early stage. After 100 h hot corrosion test, the surface of the coating was basically destroyed, there was a large area of peeling occurred on the surface of the coating. During the hot corrosion tests, the size of corrosion products continued to elongate and more different phase began to form with the extension of corrosion time.

Figure 7 shows the surface microstructure of the laser remelted TBC after hot corrosion tests. After 10 h hot corrosion test, the coating surface was still flat and smooth. With the extension of corrosion time, the obvious network cracks appeared on the surface of the coating, which attributed to the volume expansion due to the phase transition of t' -ZrO₂ to m-ZrO₂ during hot corrosion process. After 100 h hot corrosion test, the coating surface delamination was more obvious. The surface roughness of the coating increased with the cracks propagating.

Based on the cross-sectional SEM of the as-sprayed and the laser remelted TBCs after 100 h hot corrosion tests, the results suggested that a large number of holes and obvious horizontal and vertical cracks appeared

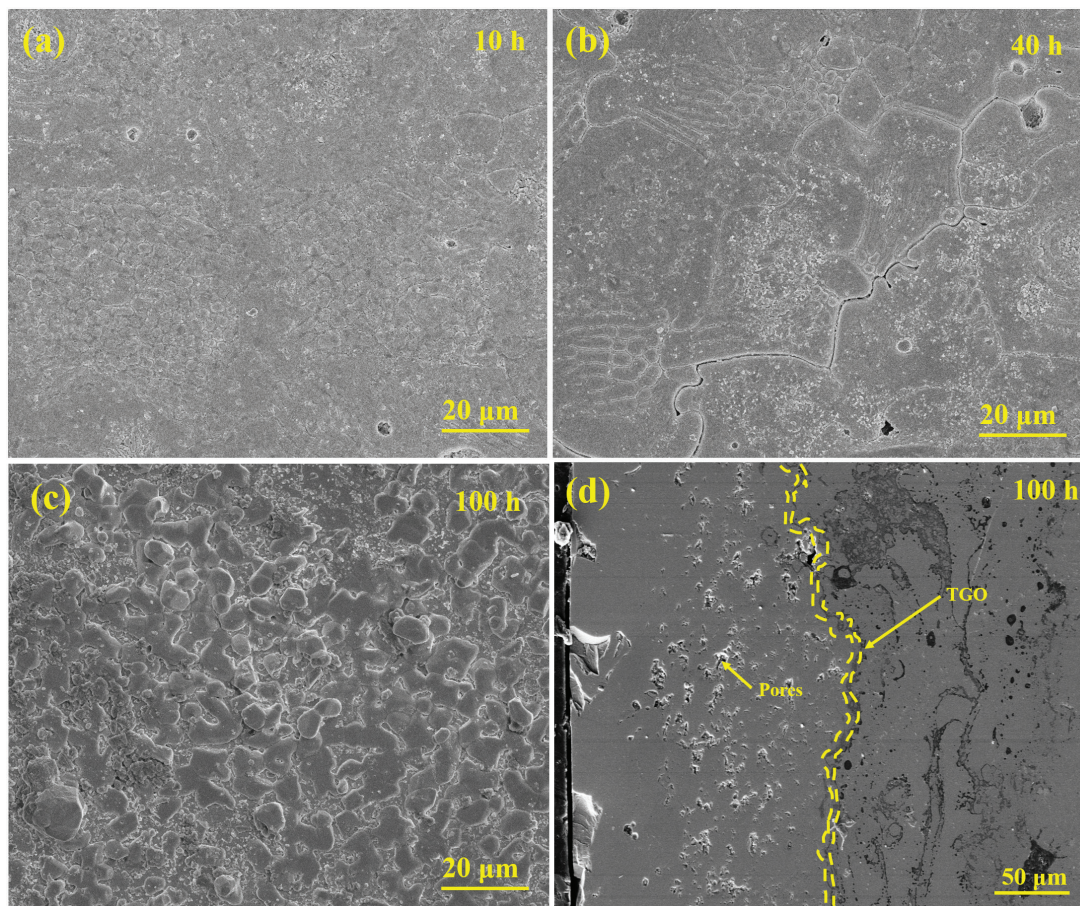


Figure 7: SEM images of the laser remelted TBC after hot corrosion test (a) 10 h (b) 40 h (c) 100 h and (d) cross-section.

in the as-sprayed TBC after hot corrosion process, the molten salts could easily diffuse into the TBC coating and react with Y element to form $Y_2(SO_4)_3$. The decrease of Y content caused the volume expansion due to the phase transition of t' - ZrO_2 to m - ZrO_2 , which also led to the crack propagation and harmed the protective coating. As for the laser remelted TBC, the number of cracks and holes was significantly reduced compared to as-sprayed TBC. The results indicated that the corrosion reaction mainly occurred on the coating surface, only few molten salts penetrated the coating and reacted with Y element. After the hot corrosion process, there were obviously continuous thermally grown oxide (TGO) appeared at the interface between the ceramic layer and the bonding layer in both as-sprayed and laser remelted TBC. However, the thickness of the TGO in the laser remelted TBC was significantly thinner than that in as-sprayed TBC. The results suggested that laser remelting treatment was beneficial to the hot corrosion resistance of the TBCs.

3.3. Hot corrosion mechanisms of as-sprayed and laser remelted TBCs

Figure 8 shows the mass change curves of as-sprayed and laser remelted TBCs after hot corrosion tests at 950 °C. The specimens of as-sprayed and laser remelted TBCs are tested in the same conditions for comparison. The results suggest that the mass gain of two types TBCs is more different during the hot corrosion tests. As for as-sprayed sample, the mass gain has a linear increment at 0–50 h hot corrosion test, which indicates that as-sprayed TBCs protect the substrate and has a good corrosion resistance. However, the mass gain has reached the maximum (2.7 mg/cm^2) at the 50 h, it can be concluded that the corrosion resistance of as-sprayed TBCs reaches its limit at this moment. Later, the mass curve declines sharply at 50–100 h, which suggests that exfoliation occurs in some areas of the top ceramic layer and the as-sprayed TBCs starts to fail. As for the laser remelted TBCs, the mass gain is lower than that of corresponding as-sprayed one during the 0–50 h hot corrosion tests, the mass gains slow at the 50–100 h hot corrosion tests. There is no mass loss during the hot corrosion tests of laser remelted sample, which suggests that no peeling occurs during the total hot corrosion process. After laser remelting treatment, the surface of TBCs is dense and exists very few porosities and cracks, which makes it difficult for molten salt to penetrate the top ceramic layer and reduces the corrosion rate during the hot corrosion

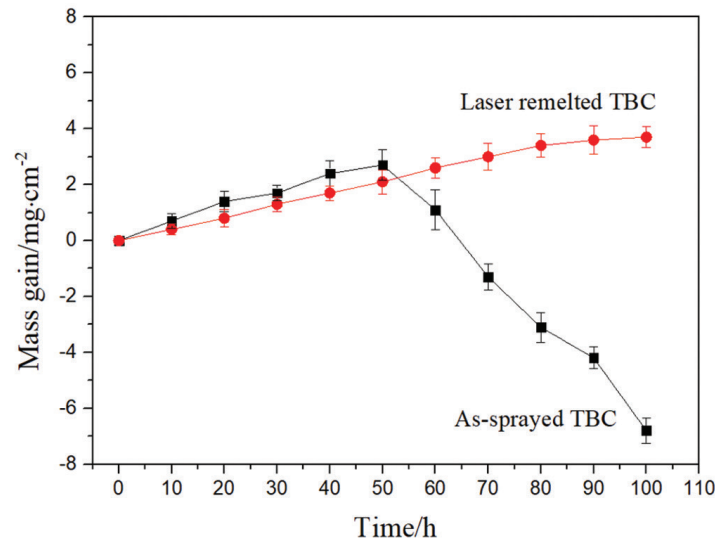


Figure 8: Mass change curves under the hot corrosion tests.

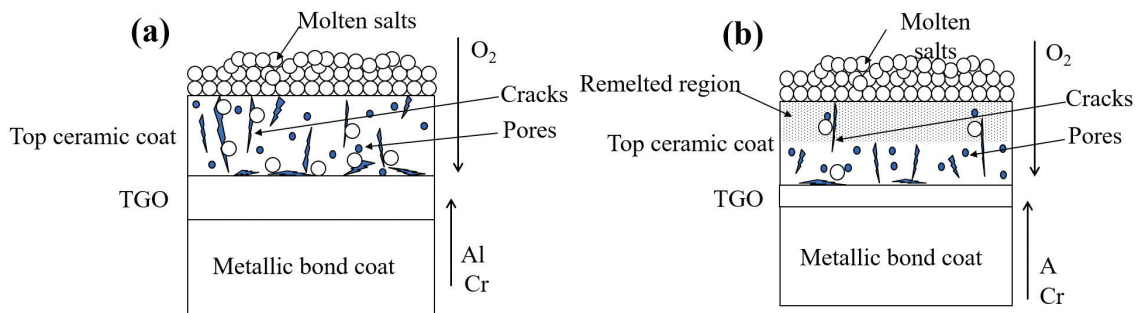


Figure 9: Schematic diagrams of (a) the as-sprayed and (b) the laser remelted TBCs during the hot corrosion tests.

tests. The mass gain is 3.8 mg/cm² at 100 h hot corrosion test. Results indicates that the laser remelted TBCs still has a certain degree of corrosion resistance in the later stage of hot corrosion.

Figure 9 illustrates the hot corrosion mechanism of the as-sprayed and laser remelted TBCs at 950 °C according to the results of SEM, XRD, microhardness and mass change curves. The damage mechanism of TBCs is complicated during hot corrosion test, which contains the high temperature oxidation and the corrosion between TBC and salts. At the beginning of hot corrosion process, the salts of NaCl and Na₂SO₄ were melted which covered the surface of the TBC to form a salt film. Then the molten salts penetrated the interior of the TBC through cracks or pores during the hot corrosion test, which promotes the consumption of Y₂O₃. The volume fraction of Y₂O₃ decreased that leads to the phase transition of t'-ZrO₂ to m-ZrO₂, which causes a volumetric expansion of TBC and cracks extension.

However, the laser remelting treatment makes the surface of TBCs densely and reduces the porosity and cracks, which is difficult for molten salt to penetrate the top ceramic layer and reduces the corrosion rate during the hot corrosion tests. The laser remelting treatment contributes to the hot corrosion resistance of TBCs at 950 °C.

4. CONCLUSIONS

In this study, NiCoCrAlY/ZrO₂-7wt%Y₂O₃ TBCs were deposited on GH4169 alloy via plasma spraying technique. Afterwards, the as-sprayed TBCs were post-treated by laser remelting process with a CO₂ laser. The two types of TBCs were exposed to hot corrosion tests at 950 °C in the presence of 75% Na₂SO₄ and 25% NaCl molten salts with 10 h, 40 h and 100 h, respectively. The results indicate that the as-sprayed TBCs have a lamellar structure with high cracks and porosity. After laser remelted treatment, the laser remelting area consists of compact sub-micro sized grains arranged in a stacked structure, which is much denser than the as-sprayed one. The microhardness and hot corrosion resistance of the laser remelted TBC are considerably better than the as-sprayed one due to the dense sub-micro sized grains arranged structure.

During the hot corrosion tests, the molten salts could easily penetrate the top ceramic layer of as-sprayed TBC and react with Y_2O_3 due to the many defects in as-sprayed TBC. The consumption of Y element promoted the phase transition of t'-ZrO₂ to m-ZrO₂, which harmed the protective coating because of the volume expansion of the phase transition. The laser remelted TBCs could significantly reduce the penetration of molten salts due to the density of the laser remelting area. The results suggest that the laser remelting treatment contributes to the hot corrosion resistance of TBCs at 950 °C.

5. ACKNOWLEDGMENTS

This project was supported by the National Natural Science Foundation of China (No. 51874185).

6. BIBLIOGRAPHY

- [1] ZHENG, H., LI, B., TAN, Y., *et al.*, “Derivative effect of laser cladding on interface stability of YSZ@Ni coating on GH4169 alloy: An experimental and theoretical study”, *Applied Surface Science*, v. 427, pp. 1105–1113, 2018.
- [2] WANG, D., TIAN, Z., WANG, S., *et al.*, “Microstructural characterization of Al₂O₃-13 wt.% TiO₂ ceramic coatings prepared by squash presetting laser cladding on GH4169 superalloy”, *Surface and Coatings Technology*, v. 254, pp. 195–201, 2014.
- [3] BARJESTEHE, M.M., ZANGENEH-MADAR, K., ABBASI, S.M., *et al.*, “The effect of platinum-aluminide coating features on high-temperature fatigue life of nickel-based superalloy”, *Journal of Mining and Metallurgy Section B-Metallurgy*, v. 55, n. 2, pp. 235–251, 2019.
- [4] DYER, S.A.S., RENÉ, M.V., DYER, P.P.O.L., *et al.*, “Study of the metallurgical bond between 316 steel substrates and NiCrAlY coating sprayed by HVOF and irradiated with a low power CO₂ laser”, *Matéria (Rio J.)*, v. 24, n. 3, e12466, 2019.
- [5] KARAOGLANLI, A.C., DOLEKER, K.M., DEMIREL, B., *et al.*, “Effect of shot peening on the oxidation behavior of thermal barrier coatings”, *Applied Surface Science*, v. 354, pp. 314–322, 2015.
- [6] BAKAN, E., VABEN, R., “Ceramic top coats of plasma-sprayed thermal barrier coatings: materials, processes, and properties”, *Journal of Thermal Spray Technology*, v. 26, n. 12, pp. 992–1010, 2017.
- [7] KARAOGLANLI, A.C., DOLEKER, K.M., OZGURLUK, Y., “State of the art thermal barrier coating (TBC) materials and tbc failure mechanisms”, *Properties and Characterization of Modern Materials*, v. 33, pp. 441–452, 2017.
- [8] OZGURLUK, Y., DOLEKER, K.M., KARAOGLANLI, A.C., “Hot corrosion behavior of YSZ, Gd₂Zr₂O₇ and YSZ/Gd₂Zr₂O₇ thermal barrier coatings exposed to molten sulfate and vanadate salt”, *Applied Surface Science*, v. 438, pp. 96–113, 2018.
- [9] CERNUSCHI, F., LORENZONI, L., CAPELLI, S., *et al.*, “Solid particle erosion of thermal spray and physical vapour deposition thermal barrier coatings”, *Wear*, v. 271, n. 11–12, pp. 2909–2918, 2011.
- [10] MORI, T., KURODA, S., MURAKAMI, H., *et al.*, “Effects of initial oxidation on β phase depletion and oxidation of CoNiCrAlY bond coatings fabricated by warm spray and HVOF processes”, *Surface and Coatings Technology*, v. 221, pp. 59–69, 2013.
- [11] GORAL, M., SWAD'ZBA, R., KUBASZEK, T., “TEM investigations of TGO formation during cyclic oxidation in two- and three-layered thermal barrier coatings produced using LPPS, CVD and PS-PVD methods”, *Surface and Coatings Technology*, v. 394, e125875, 2020.
- [12] GORAL, M., KOTOWSKI, S., NOWOTNIK, A., *et al.*, “PS-PVD deposition of thermal barrier coatings”, *Surface and Coatings Technology*, v. 237, pp. 51–55, 2013.
- [13] MAUER, G., JARLIGO, M.O., REZANKA, S., *et al.*, “Novel opportunities for thermal spray by PS-PVD”, *Surface and Coatings Technology*, v. 268, pp. 52–57, 2015.
- [14] WANG, Y., DARUT, G., POIRIER, T., *et al.*, “Ultrasonic cavitation erosion of as-sprayed and laser-remelted yttria stabilized zirconia coatings”, *Journal of the European Ceramic Society*, v. 37, n. 11, pp. 3623–3630, 2017.
- [15] ZHANG, X.F., ZHOU, K.S., DONG, S.J., *et al.*, “Effect of Al-deposition on erosion resistance of plasma sprayed thermal barrier coating”, *Transactions of Nonferrous Metals Society of China*, v. 25, n. 8, pp. 2587–2593, 2015.
- [16] ZHANG, X.F., NIU, S.P., DENG, Z.Q., *et al.*, “Preparation of Al₂O₃ nanowires on 7YSZ thermal barrier coatings against CMAS corrosion”, *Transactions of Nonferrous Metals Society of China*, v. 29, n. 11, pp. 2362–2370, 2019.

- [17] YANG, K., LI, J., WANG, Q., *et al.*, “Effect of laser remelting on microstructure and wear resistance of plasma sprayed Al₂O₃-40%TiO₂ coating”, *Wear*, v. 426–467, pp. 314–318, 2019.
- [18] JIANBING, Y., WANG, Y., ZHOU, F., *et al.*, “Laser remelting of plasma-sprayed nanostructured Al₂O₃–20 wt.% ZrO₂ coatings onto 316l stainless steel”, *Applied Surface Science*, v. 431, pp. 112–121, 2018.
- [19] YANG, E.J., LUO, X.T., YANG, G.J., *et al.*, “A TEM study of the microstructure of plasma-sprayed YSZ near inter-splat interfaces”, *Journal of Thermal Spray Technology*, v. 24, n. 6, pp. 907–914, 2015.
- [20] SOBHANVERDI, R., AKBARI, A., “Porosity and microstructural features of plasma sprayed Yttria stabilized Zirconia thermal barrier coatings”, *Ceramics International*, v. 41, n. 10, pp. 14517–14528, 2015.
- [21] CUI, S., HUANG, J., LUO, J., *et al.*, “Evaluation of a sealed layer on a porous thermal barrier coating against molten calcium–magnesium–alumina–silicate corrosion”, *Materials and Design*, v. 208, e109918, 2021.
- [22] BATISTA, C., PORTINHA, A., RIBEIRO, R.M., *et al.*, “Morphological and microstructural characterization of laser-glazed plasma-sprayed thermal barrier coatings”, *Surface and Coatings Technology*, v. 200, n. 9, pp. 2929–2937, 2006.
- [23] DOLEKER, K.M., OZGURLUK, Y., KAHRAMAN, Y., *et al.*, “Oxidation and hot corrosion resistance of HVOF/EB-PVD thermal barrier coating system”, *Surface and Coatings Technology*, v. 409, n. 15, e126862, 2021.
- [24] QUAZI, M.M., FAZAL, M.A., HASEEB, A.S.M.A., *et al.*, “Laser-based surface modifications of aluminum and its alloys”, *Critical Reviews in Solid State and Materials Sciences*, v. 41, n. 2, pp. 106–131, 2016.
- [25] VASSEN, R., STUKE, A., STOVER, D., “Recent developments in the field of thermal barriercoatings”, *Journal of Thermal Spray Technology*, v. 18, n. 2, pp. 181–186, 2009.